Melanoma Diagnosis

International Edition: DOI: 10.1002/anie.201509397
German Edition: DOI: 10.1002/ange.201509397

Monitoring Tyrosinase Expression in Non-metastatic and Metastatic Melanoma Tissues by Scanning Electrochemical Microscopy

*Tzu-En Lin, Alexandra Bondarenko, Andreas Lesch, Horst Pick, Fernando Cortés-Salazar, and Hubert H. Girault**

Abstract: *Although tremendous progress has been made in the diagnosis of melanoma, the identification of different stages of malignancy in a reliable way remains challenging. Current strategies rely on optical monitoring of the concentration and spatial distribution of specific biomarkers. State-of-the-art optical methods can be affected by background-color interference and autofluorescence. We overcame these shortcomings by employing scanning electrochemical microscopy (SECM) to map the prognostic indicator tyrosinase (TyR) in non-metastatic and metastatic melanoma tissues by using soft-stylus microelectrodes. Electrochemical readout of the TyR distribution was enabled by adapting an immunochemical method. SECM can overcome the limitations of optical methods and opens unprecedented possibilities for improved diagnosis and understanding of the spatial distribution of TyR in different melanoma stages.*

Melanoma is one of the most lethal cutaneous malignancies, and strikes about 132 000 people per year worldwide.[1] Earlier stages of melanoma (stages 0, I and II) can be cured. However, the survival rate decreases drastically for metastatic melanoma (stages III and IV) because the cancer has already invaded the lymph nodes and other organs.[2] Consequently, surgery and adjuvant therapies including immunotherapy or chemotherapy may be applied. Reliable methods for the unequivocal identification of cancer metastasis are of high relevance. The similar appearance of melanoma and innocuous skin moles impedes easy cancer identification. The prevalent method to confirm malignancy is based on the detection of specific biomarkers on biopsies by immunohistochemistry (IHC) combined with pathological analysis. In IHC, biomarkers are typically visualized optically by immunoassays with functionalized labels (e.g., horse radish peroxidase (HRP) or fluorescent tagging molecules). However, optical methods often suffer from practical limitations that potentially lead to uncertain conclusions. For instance, melanin can resemble the color of the chromogen 3,3′-diaminobenzidine (DAB), which is commonly employed in IHC (Figure S1 in the Supporting Information).[3] Alternatively, fluorescent tagging could be impeded by cellular autofluorescence or photobleaching.[4]

Electrochemical methods may represent a promising alternative since they rely exclusively on the electrochemical detection of redox-active species related to the presence of biomarkers. Scanning electrochemical microscopy (SECM) is a surface reactivity mapping tool with high spatial resolution and sensitivity that has been used widely for studying living cell cultures[5] but rarely for tissues. For instance, enzymatic activity and oxygen production/consumption in plant tissues and microtissues have been monitored.[6] SECM has also been applied to study molecular transport through skin samples.[7] The lateral dimensions of tissue samples can approach square centimeters and height differences can be in the critical domain of the SECM probe. Since the probe–sample interaction depends on the working distance d data interpretation from uneven samples can become cumbersome. An uncontrolled d can lead to probe–sample crashes when scanning closely over a tissue, leading to irreparable damage to the specimens and contamination of the sensing probe. The former is especially true when using microelectrodes (ME) enclosed in a hard insulating glass body.

In this work, we present SECM for precise mapping of the tyrosinase (TyR) distribution in formalin-fixed, paraffin-embedded tissue microarrays (TMA) of skin biopsies taken from nine patients. TyR is a copper-containing enzyme that controls the production of melanin,[8] and it can be used as a highly selective indicator for the prognostic diagnosis of melanoma.[9] Recently, this has been demonstrated for biopsy samples analyzed in an electrochemical biosensor platform.[10] In this work, an immunodetection strategy for TyR was adapted for the monitoring of melanoma stages through the electrochemical detection of TMB_{ox}, which is the enzymatic reaction product of tetramethylbenzidine (TMB), H_2O_2, and HRP (Scheme 1 a).[11] Soft ME probes capable of scanning delicate samples with topographic sample features in a gentle brush-like contact mode and at constant d were employed (Scheme 1 b).[12] These soft SECM probes were previously introduced by our group for simple and affordable constant-distance control. Alternative approaches require the combination of SECM with technically and experimentally sophisticated distance-control tools.[5b,13]

Figure 1 a shows SECM line scans over skin biopsy sections from three different patients containing melanoma stages II (non-metastatic) and III (metastatic), and normal skin tissues. A conventional Pt ME in constant-height mode

[*] T.-E. Lin, A. Bondarenko, A. Lesch, F. Cortés-Salazar, Prof. H. H. Girault
Laboratoire d'Electrochimie Physique et Analytique
École Polytechnique Fédérale de Lausanne, EPFL Valais Wallis
CH-1951 Sion (Switzerland)
E-mail: hubert.girault@epfl.ch
H. Pick
Laboratory of Physical Chemistry of Polymers and Membranes
École Polytechnique Fédérale de Lausanne
CH-1015 Lausanne (Switzerland)

Supporting information and ORCID(s) from the author(s) for this article are available on the WWW under http://dx.doi.org/10.1002/anie.201509397.

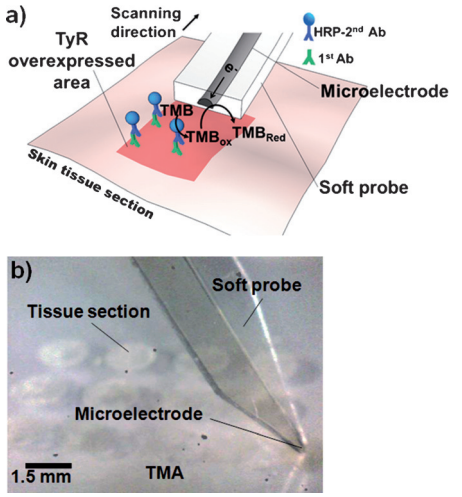

Scheme 1. a) Schematic representation of the immunoassay-based detection strategy to map the TyR distribution in tissue sections by using a soft SECM probe and TMB as the redox-active species. b) Photograph of a soft probe when scanning over a TMA.

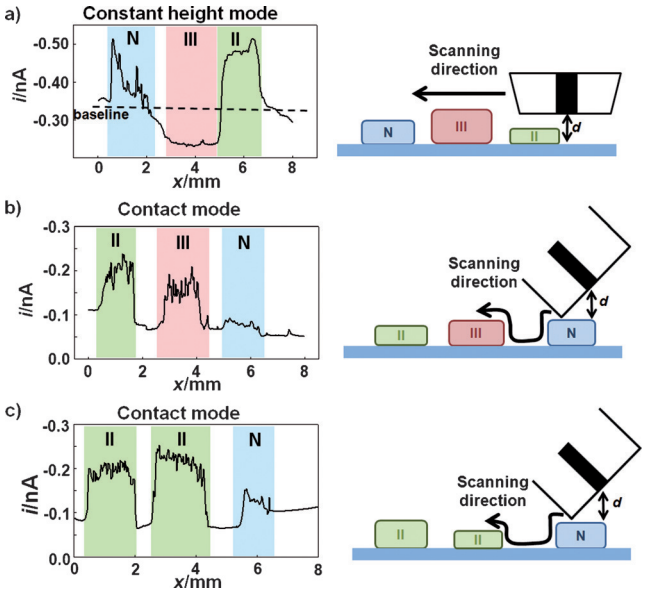

Figure 1. SECM line scans in constant-height mode using a conventional microelectrode (a) and in contact mode with a soft SECM probe (b, c) over a TMA containing normal skin (blue, N), stage II melanoma (green, II) and stage III melanoma (red, III) melanoma tissue sections. Each tissue section was from a different patient. The panels on the right illustrate the two scanning modes.

was employed by adjusting *d* with respect to the glass support of the TMA and not to the tissue surface (experimental details in Section SI-2; line scan directions in Figure S3). The highest expression level of TyR was observed in stage II tissue samples. A lower level of TyR was found in normal skin, where TyR is produced at moderate levels by melanocytes located in the bottom layer of the epidermis. As it can be seen in Figure 1 a, over the stage III tissue section, much lower currents than the baseline current (defined as the hindered diffusion current measured over the insulating glass substrate) were detected. Diffusion of the redox-active species towards the ME was significantly blocked owing to a very small *d* over the relatively thick stage III tissue. This observation is supported by topographic measurements of the tissue samples recorded in a hydrated state in the experimental solution (Figure S4). Stage III samples showed stronger swelling and thus a more pronounced height. As a result, correct interpretation of the measured constant height SECM data over a TMA is challenging. Therefore, tissue sections can only be investigated individually in contactless mode by adjusting *d* subsequently over each section (Figure S5). Moreover, constant-height-mode scanning over such large samples can induce microscratches or partially detached tissue material upon a mechanical ME–tissue contact (Figure S6).

To overcome these drawbacks, soft-stylus probes (see Section SI-2) were employed for the contact-mode scanning of biopsies from another six patients (Figure 1 b, c and Figure S3). It is worth mentioning that the tissue sections were not damaged during the contact-mode scanning thanks to the weak forces exerted by the soft probe on the sample (Figure S7).[14] In addition, all six tissue sections and the obtained data demonstrate the reproducibility of the SECM approach among samples from different persons. The different TyR levels (stage II > normal skin) were identified with high certainty and sensitivity. Stage III melanoma shows a slightly lower TyR content over the entire tissue section than stage II. It has been reported previously that the TyR distribution in stage III melanoma is heterogeneous,[11b] and in consequence, single SECM line scans are not representative.

Therefore, SECM images of normal skin, as well as of melanoma stages II and III sections, were recorded and compared with tissues examined by the conventional IHC method (Figure 2). The SECM image in Figure 2 a clearly indicates a homogeneous overexpression of TyR in stage II and a heterogeneous distribution in stage III melanoma. Tumors tend to develop different mechanisms of immunosuppression to avoid being destroyed by the immune system.[15] Shedding or mutation of the tumor antigens is one strategy that facilitates tumor escape from the immune system, leading to tumor proliferation and metastasis. As a tumor-associated antigen, TyR is recognized by the immune system and thus a gradual loss of TyR could be of benefit for tumor escape. As a consequence, the TyR distribution is heterogeneous and slightly decreased in stage III melanoma in accordance with our presented data. In normal skin tissue, the TyR content increased slightly towards the basal epidermis, where normal melanocytes are located. The observed polarity of TyR distribution is in agreement with reports in the literature.[11b] Because other TyR distribution patterns than the one shown are known to be a sign of different TyR-related dermal diseases, the presented SECM approach could provide further screening applications. The specificity of the TyR immunoassay was confirmed by applying the method without primary antibodies (Abs), which showed an insignificant contribution from non-specific binding (Figure S8). In conventional IHC, TyR is labeled with a specific pink chromogen (Section SI-2) and thus its detection is strongly interfered with

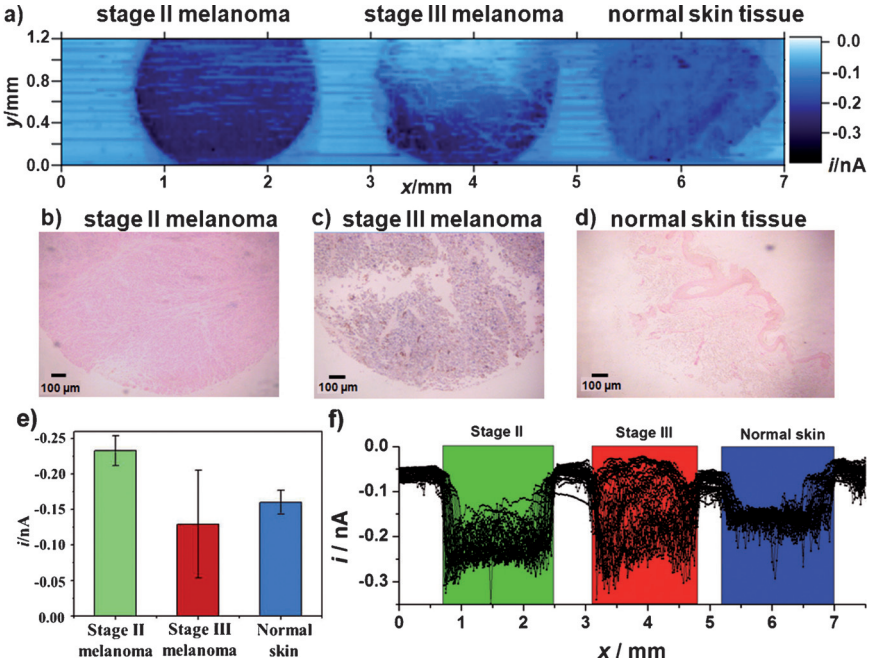

Figure 2. a) Contact-mode SECM image of stage II and stage III melanoma and normal skin tissues after immunostaining of TyR. b–d) Optical images of tissues obtained by IHC. Similar but different tissue samples were used in (a) and (b–d), respectively. TyR was stained in pink. e) Average currents of normal skin and stage II and stage III melanomas. Nine current values were extracted and averaged from each tissue section. f) 2D plot of all line scans of the SECM image in Figure 2a.

by melanin in stage III melanoma (Figure 2c). By contrast, the electrochemical detection of TyR by SECM is not affected by colored background samples (Figures S1, S7).

The importance of mapping the local TyR distribution becomes apparent when averaging the currents from nine representative locations in each tissue section to reflect the global TyR concentration (see Figure S9). In the column plot in Figure 2e, Stage II melanoma shows the highest average current, followed by normal skin and stage III melanoma. Hence, the lower currents for stage III melanoma could be interpreted wrongly as normal skin. However, as can be seen from the SECM image and its 2D plot (Figure 2f), the lower average current for stage III is a result of heterogeneous TyR distribution. Locally, the SECM currents were higher than in stage II. SECM imaging visualizes the abnormal distribution of the TyR (not in the basal layer of epidermis) and confirms the correct identification of stage III melanoma tissue samples. This shows the limitation of traditional sensors that only measure the global concentration of a certain biomarker, while demonstrating the advantage of spatial resolution. Discrimination between stage II and stage III melanoma is of high relevance because it drastically influences the medical treatment in terms of chemotherapy, immunotherapy, or TyR DNA vaccine therapy (Section SI-10).[16]

In conclusion, SECM on skin biopsies from different melanoma patients allows accurate monitoring of TyR expression and distribution in distinct melanoma stages. An immunoassay was employed to distinguish melanoma stages II and III by using soft SECM probes for gentle contact-mode brushing of the delicate tissue samples. The progression from a homogeneous TyR distribution in stage II to a heterogeneous one in stage III was clearly visualized and in comparison with IHC, the SECM concept is not limited by the presence of optically interfering species, such as melanin. Hence, SECM mapping of TyR might be implemented directly or as a complementary prognostic technique for diagnosing metastatic and non-metastatic melanoma stages. Soft ME arrays will accelerate the analysis to screen cancer tissue libraries of clinically relevant quantities.[14b,17] Furthermore, the integration of microfluidic channels into the soft probe could enable advanced control of the surrounding tissue microenvironment for simultaneous electrochemical, fluorescence, and mass spectrometry detection.[18]

Acknowledgements

T.-E. Lin thanks the Taiwanese Ministry of Education (MOE) for the 2013 MOE Technologies Incubation Scholarship and Dr. Chi-Lin Li (National Taiwan University) for the support in preparing Scheme 1a. The SNSF (Switzerland) and the UEFISCDI (Romania) are thanked for the support throughout project no. IZERZO_142236/1.

Keywords: melanoma · scanning electrochemical microscopy · soft probes · tissue sections · tyrosinase

How to cite: *Angew. Chem. Int. Ed.* **2016**, *55*, 3813–3816
Angew. Chem. **2016**, *128*, 3878–3881

[1] J.-S. Taylor, *Science* **2015**, *347*, 824.
[2] a) V. Gray-Schopfer, C. Wellbrock, R. Marais, *Nature* **2007**, *445*, 851–857; b) B. E. G. Rothberg, M. B. Bracken, D. L. Rimm, *J. Natl. Cancer Inst.* **2009**, *101*, 452–474.
[3] a) M. N. Bobrow, K. J. Shaughnessy, G. J. Litt, *J. Immunol. Methods* **1991**, *137*, 103–112; b) C. Cao, S. J. Sim, *Biosens. Bioelectron.* **2007**, *22*, 1874–1880; c) S. Zhang, J. Yang, J. Lin, *Bioelectrochemistry* **2008**, *72*, 47–52.
[4] M. Monici, *Biotechnol. Annu. Rev.* **2005**, *11*, 227–256.
[5] a) B. Liu, S. A. Rotenberg, M. V. Mirkin, *Proc. Natl. Acad. Sci. USA* **2000**, *97*, 9855–9860; b) Y. Takahashi, A. I. Shevchuk, P. Novak, B. Babakinejad, J. Macpherson, P. R. Unwin, H. Shiku, J. Gorelik, D. Klenerman, Y. E. Korchev, *Proc. Natl. Acad. Sci. USA* **2012**, *109*, 11540–11545; c) M. Nebel, S. Grützke, N. Diab, A. Schulte, W. Schuhmann, *Angew. Chem. Int. Ed.* **2013**, *52*, 6335–6338; *Angew. Chem.* **2013**, *125*, 6460–6463; d) S. Rapino, R. Marcu, A. Bigi, A. Soldà, M. Marcaccio, F. Paolucci, P. G. Pelicci, M. Giorgio, *Electrochim. Acta* **2015**, *179*, 65–73.
[6] a) L. Gac, A. Sridhar, H. L. D. Boer, A. V. D. Berg, *PLoS One* **2014**, *9*, e93618; b) A. Sridhar, A. V. D. Berg, S. Le, *Electroanalysis* **2014**, *26*, 1881–1885; c) R. Zhu, S. M. Macfie, Z. Ding,

J. Exp. Bot. **2005**, *56*, 2831 – 2838; d) M. Tsionsky, Z. G. Cardon, A. J. Bard, R. B. Jackson, *Plant Physiol.* **1997**, *113*, 895 – 901; e) H. Zhou, H. Shiku, S. Kasai, H. Noda, T. Matsue, H. Ohya-Nishiguchi, H. Kamada, *Bioelectrochemistry* **2001**, *54*, 151 – 156.

[7] a) B. D. Bath, R. D. Lee, H. S. White, E. R. Scott, *Anal. Chem.* **1998**, *70*, 1047 – 1058; b) E. R. Scott, H. S. White, J. B. Phipps, *Anal. Chem.* **1993**, *65*, 1537 – 1545.

[8] a) L. Xiao, K. Matsubayashi, N. Miwa, *Arch. Dermatol. Res.* **2007**, *299*, 245 – 257; b) V. J. Hearing, K. Tsukamoto, *FASEB J.* **1991**, *5*, 2902 – 2909.

[9] G. E. Orchard, *Histochem. J.* **2000**, *32*, 475 – 481.

[10] M. Mossberg, S. Vernick, R. Ortenberg, G. Markel, Y. Shacham-Diamand, J. Rishpon, *Electroanalysis* **2014**, *26*, 1671 – 1675.

[11] a) J. L. Boyle, H. M. Haupt, J. B. Stern, H. A. B. Multhaupt, *Arch. Pathol. Lab. Med.* **2002**, *126*, 816 – 822; b) G. F. L. Hofbauer, J. Kamarashev, R. Geertsen, R. Böni, R. Dummer, *J. Cutaneous Pathol.* **1998**, *25*, 204 – 209; c) M. Urosevic, B. Braun, J. Willers, G. Burg, R. Dummer, *Exp. Dermatol.* **2005**, *14*, 491 – 497; d) T.-E. Lin, F. Cortés-Salazar, A. Lesch, L. Qiao, A. Bondarenko, H. H. Girault, *Electrochim. Acta* **2015**, *179*, 57 – 64.

[12] a) F. Cortés-Salazar, M. Träuble, F. Li, J.-M. Busnel, A.-L. Gassner, M. Hojeij, G. Wittstock, H. H. Girault, *Anal. Biochem.* **2009**, *81*, 6889 – 6896; b) A. Lesch, D. Momotenko, F. Cortés-Salazar, F. Roelfs, H. H. Girault, G. Wittstock, *Electrochim. Acta* **2013**, *110*, 30 – 41.

[13] a) J. V. Macpherson, P. R. Unwin, *Anal. Chem.* **2000**, *72*, 276 – 285; b) B. B. Katemann, A. Schulte, W. Schuhmann, *Chem. Eur. J.* **2003**, *9*, 2025 – 2033; c) T. H. Treutler, G. Wittstock, *Electrochim. Acta* **2003**, *48*, 2923 – 2932; d) A. G. Güell, N. Ebejer, M. E. Snowden, J. V. Macpherson, P. R. Unwin, *J. Am. Chem. Soc.* **2012**, *134*, 7258 – 7261; e) C. Kranz, G. Friedbacher, B. Mizaikoff, A. Lugstein, J. Smoliner, E. Bertagnolli, *Anal. Chem.* **2001**, *73*, 2491 – 2500.

[14] a) A. Lesch, D. Momotenko, F. Cortés-Salazar, I. Wirth, U. M. Tefashe, F. Meiners, B. Vaske, H. H. Girault, G. Wittstock, *J. Electroanal. Chem.* **2012**, *666*, 52 – 61; b) A. Lesch, B. Vaske, F. Meiners, D. Momotenko, F. Cortés-Salazar, H. H. Girault, G. Wittstock, *Angew. Chem. Int. Ed.* **2012**, *51*, 10413 – 10416; *Angew. Chem.* **2012**, *124*, 10559 – 10563.

[15] a) P. Alexander, *Cancer Res.* **1974**, *34*, 2077 – 2082; b) F. H. Igney, P. H. Krammer, *J. Leukocyte Biol.* **2002**, *71*, 907 – 920.

[16] J. Yan, C. Tingey, R. Lyde, T. C. Gorham, D. K. Choo, A. Muthumani, D. Myles, L. P. Weiner, K. A. Kraynyak, E. L. Reuschel, T. H. Finkel, J. J. Kim, N. Y. Sardesai, K. E. Ugen, K. Muthumani, D. B. Weiner, *Cancer Gene Ther.* **2014**, *21*, 507 – 517.

[17] F. Cortés-Salazar, D. Momotenko, H. H. Girault, A. Lesch, G. Wittstock, *Anal. Chem.* **2011**, *83*, 1493 – 1499.

[18] a) A. Bondarenko, F. Cortés-Salazar, M. Gheorghiu, S. Gáspár, D. Momotenko, L. Stanica, A. Lesch, E. Gheorghiu, H. H. Girault, *Anal. Chem.* **2015**, *87*, 4479 – 4486; b) D. Momotenko, F. Cortés-Salazar, A. Lesch, G. Wittstock, H. H. Girault, *Anal. Chem.* **2011**, *83*, 5275 – 5282.

Received: October 8, 2015
Revised: December 2, 2015
Published online: February 5, 2016

